The self-consistent ground state of the two-dimensional electron gas

1998 J. Phys.: Condens. Matter 10 821

(http://iopscience.iop.org/0953-8984/10/4/011)

J. Phys.: Condens. Matter **10** (1998) 821–832. Printed in the UK PII: S0953-8984(98)85718-4

The self-consistent ground state of the two-dimensional electron gas

M Moreno†, R M Méndez-Moreno‡ and S Orozco‡

† Instituto de Física, Universidad Nacional Autónoma de México, Apartado Postal 20-364, 01000 México, DF, Mexico

‡ Departamento de Física, Facultad de Ciencias, Universidad Nacional Autónoma de México, Apartado Postal 21-092, 04021 México, DF, Mexico

Received 3 July 1997, in final form 28 October 1997

Abstract. The self-consistent Hartree–Fock approximation and the deformable jellium model are used to describe the ground state of the two-dimensional electron gas. Improved precision in the calculations allows us to confirm the existence of a *stable* corrugated state at finite densities. This is strongly corroborated by an extrapolation of our results to the low-density region. A positive bulk modulus is obtained in this region. A comparison with experimental data for the melting point and our model calculation is made and agreement is found within a factor of 2.

1. Introduction

The properties of the two-dimensional electron gas (2DEG) have attracted considerable interest in the past few years [1]. In particular, because the electronic motion in the new high-temperature superconducting materials occurs mostly in planes, the 2DEG has become a subject of intensive research, both theoretical and experimental [2]. More relevant for us is that the studies of two-dimensional (2D) fermion systems are useful for understanding the surfaces of three-dimensional solids and interfaces of three-dimensional phases [3]. Thus experiments with the 2DEG have produced strong evidence for an electron solid in the quantum regime even in zero magnetic field [4–6]. Since this transition to the crystalline phase has been established, it is important to carry out a better determination of the theoretical conditions under which this crystallization occurs. Most standard studies of the electron gas assume a simplified model for the neutralizing positive background [7]. A common approximation is the uniform jellium model (UJ) in which the system of electrons interacting with each other via the Coulomb potential are immersed in a uniform static neutralizing positive background. The UJ provides an important theoretical approach which requires only one input parameter, namely the average electron density in the bulk, r_s, to describe the properties of the 2DEG at zero magnetic field and temperature [8–10].

A different hypothesis for the positive background is the deformable jellium model (DJ), first introduced by Overhauser [11, 12]. The basic assumption in this model is that the background is statically deformed in order to get local charge neutrality, simulating some of the expected properties of the system. Physically, the DJ can be viewed as a way to incorporate some screening effects [13]. The DJ retains the simplicity of the UJ and the properties depend only on the Wigner–Seitz parameter r_s. It can be argued that the DJ should be applicable in the low-density region, where the positive-ion repulsion can be neglected

0953-8984/98/040821+12$19.50

as for a low-density gas. Calculations of the electron gas at zero magnetic field in the DJ within the self-consistent Hartree–Fock (HF) approximation show that the electronic part of the system develops long-range order in the form of electron-density waves (eDW) of the Wigner type at low densities [12]. An achievement of including the electron gas in the DJ is the systematic description of the symmetry transition from the homogeneous phase at high densities into localized states at low densities. The DJ together with the self-consistent HF approximation have been exploited by us to describe the electron gas [14, 15]. In previous work the existence of a stable corrugated state was found. However, the limitations of the calculation for the low-density region, $r_s > 25$, left serious doubts about the nature of the stability of the corrugated state.

In this work the ground-state properties of the 2DEG in the HF-DJ model are studied at zero magnetic field. In order to find electron localization, an expansion for the state function of the type of the eDW is proposed. A considerably reduced matrix is obtained when *symmetries of the state function* can be explicitly introduced. This reduction allows us to deal with a great number of terms in the expansion at a small fraction of the computational burden. The convergence of the energy is carefully studied as a function of the number of terms in the expansion at intermediate and low densities. Then an extrapolation is performed to very low densities (large values of r_s), and the existence of a stable localized state at finite densities is confirmed for the paramagnetic and the ferromagnetic phases. Positive pressure and bulk modulus are obtained for this region. The electron density $\rho(r_s)$ for two different r_s-values is calculated. We compare our results with other model predictions and also with the zero-magnetic-field experiments on the Wigner crystal melting point. Atomic units are used throughout this work, with the energy in rydbergs.

2. The model

Let us consider a system of N fermions interacting via a Coulomb potential $\hat{V}(r_{ij}) = e^2/r_{ij}$ with $r_{ij} = |\boldsymbol{r_i} - \boldsymbol{r_j}|$, immersed in a positive background of area A. When the thermodynamic limit is considered, $N \to \infty$ and $A \to \infty$ with $\sigma = N/A$ constant.

The HF Hamiltonian of the electron gas in jellium has the terms

$$\hat{H}_{HF} = \sum_{i=1}^{N} \frac{\hat{p}_i^2}{2m_e} + \hat{V}_D + \hat{V}_{ex} + \hat{V}_{bb} + \hat{V}_{be} \tag{1}$$

where the subscripts e and b refer to electron and background, respectively, and $\hat{V}_D$ and $\hat{V}_{ex}$ are the direct and exchange terms of the electron–electron interaction respectively.

The deformable jellium is defined by the condition [16, 13, 17]

$$\langle \hat{V}_D \rangle + \langle \hat{V}_{bb} \rangle + \langle \hat{V}_{be} \rangle = 0 \tag{2}$$

where the symbol $\langle\ \rangle$ means the expectation value with respect to the ground state. This condition means that the positive background is statically deformed in order to achieve local charge neutrality of the system; in the independent-particle approximation the background density *follows* the electron density. In order to evaluate the energy, we are left just with the electronic kinetic and the exchange energy terms.

The trial functions in the Fock space are taken to be

$$\Phi^i = \sum_{j=0}^{M} C_j^i \phi_j. \tag{3}$$

If due to some symmetries of the basis and *the physical state* (not necessarily of the Hamiltonian), the index j can be separated into two or more different indices that can be summed independently, i.e. $j = (L, N)$, then equation (3) can be rewritten as

$$\Phi^i = \sum_{L=0}^{\mathcal{L}} \sum_{N=0}^{\mathcal{N}} C^i_{L,N} \phi_{L,N} = \sum_{L=0}^{\mathcal{L}} C^i_{L,N_0} \left\{ \sum_{N=0}^{\mathcal{N}} \frac{C^i_{L,N}}{C^i_{L,N_0}} \phi_{L,N} \right\}$$

where the factor $C^i_{L,N}/C^i_{L,N_0} \equiv b_{L,N}$ is usually independent of the parameter r_s.

From the orthonormality of the orbitals,

$$\left\langle \sum_{N=0}^{\mathcal{N}} b_{L,N} \phi_{L,N} \middle| \sum_{N'=0}^{\mathcal{N}} b_{L,N'} \phi_{L,N'} \right\rangle = \sum_{N=0}^{\mathcal{N}} |b_{L,N}|^2 = \mathcal{N}_L^2.$$

Using the above results, the reduced equation for the orbitals is

$$\Phi^i = \sum_{L=0}^{\mathcal{L}} \left[C^i_{L,N_0} \mathcal{N}_L \right] \left[\frac{1}{\mathcal{N}_L} \sum_{N=0}^{\mathcal{N}} b_{L,N} \phi_{L,N} \right] = \sum_{L=0}^{\mathcal{L}} \mathcal{C}^i_{L,N_0} \Omega_L. \tag{4}$$

In equation (4) the sum over the index N can be independently evaluated for each value of L. We have $\mathcal{C}^i_{L,N_0} = C^i_{L,N_0} \mathcal{N}_L$ and

$$\Omega_L = \frac{1}{\mathcal{N}_L} \sum_{N=0}^{\mathcal{N}} b_{L,N} \phi_{L,N}.$$

Then using equation (4) for the expansion of the orbitals, the number of terms in the sum over L is considerably reduced with respect to the initial sum in equation (3). Therefore the number of independent coefficients to be evaluated, and the dimensions of the matrices involved in the calculations are significantly diminished. The price of this reduction in the matrix dimensionality is an increase in the complexity of the matrix elements. However, this complexity can be controlled by taking advantage of symmetry properties of the matrix elements when the summation over the index N is performed. In that way the calculations with the expansion given by equation (4) are simpler and more economic for given computational resources. This procedure amounts to a change of the variational basis, from Φ to Ω orbitals; the conditions that it imposes imply in general that some of the excited electronic states with different orbital symmetries are excluded from the variational calculation. Because in this work we are interested in the ground state, this constraint is not relevant.

The above discussion is illustrated now with the selection of the orbitals in this work. The expansion proposed is given in terms of a set of modulating functions that contain as a possible solution the trivial plane wave (PW). The general form is given by

$$\Phi_{\boldsymbol{k}}(\boldsymbol{r}) = \frac{\exp(\mathrm{i}\boldsymbol{k} \cdot \boldsymbol{r})}{\sqrt{A}} \sum_{n_x=-\mathcal{N}}^{\mathcal{N}} \sum_{n_y=-\mathcal{N}}^{\mathcal{N}} C'_{n_x,n_y} [\exp(\mathrm{i}q_0 n_x x) \exp(\mathrm{i}q_0 n_y y)]. \tag{5}$$

A is the area in which the periodic boundary conditions are imposed, $\boldsymbol{k} = \hat{\boldsymbol{i}} k_x + \hat{\boldsymbol{j}} k_y$, and $\boldsymbol{r} = \hat{\boldsymbol{i}} x + \hat{\boldsymbol{j}} y$. The coefficients C'_{n_x,n_y} in the expansion, assumed to be independent of $\boldsymbol{k}$, are self-consistently determined. The minimal modulating frequency $q_0 = 2k_F$ with k_F the Fermi momentum, is obtained via the orthonormality condition for the orbitals. The term with $n_x = n_y = 0$ is the PW solution. The number of terms in the expansion for the state function is $(2\mathcal{N} + 1)^2$.

Because the coefficients in the expansion for the ground-state equation (5) satisfy the property $C'_{n_x,n_y} = C'_{-n_x,n_y} = C'_{n_x,-n_y} = C'_{-n_x,-n_y}$, the expansion of the state function can be written in terms of a cosine series as

$$\Phi_{\boldsymbol{k}}(\boldsymbol{r}) = \frac{\exp(\mathrm{i}\boldsymbol{k}\cdot\boldsymbol{r})}{\sqrt{A}} \sum_{n_x=0}^{\mathcal{N}} \sum_{n_y=0}^{\mathcal{N}} C''_{n_x,n_y} [\cos(q_0 n_x x)\cos(q_0 n_y y)]. \tag{6}$$

The number of terms in the above expansion is $(\mathcal{N}+1)^2$. Then summing over the negative values of the indices is not necessary with the use of the new functions. If now the equivalence of the directions $\boldsymbol{x}$ and $\boldsymbol{y}$ for *the ground state* is taken into account, expansion (6) can be further simplified to

$$\Phi_{\boldsymbol{k}}(\boldsymbol{r}) = \frac{\exp(\mathrm{i}\boldsymbol{k}\cdot\boldsymbol{r})}{\sqrt{A}} \sum_{n_x=0}^{\mathcal{N}} \sum_{n_y=0}^{n_x} C_{n_x,n_y} \mathcal{P}_{n_x,n_y} [\cos(q_0 n_x x)\cos(q_0 n_y y)] \tag{7}$$

where $\mathcal{P}_{n_x,n_y}$ is an operator that sums all the permutations of the subscripts n_x and n_y. The number of terms in the expansion for the state function is now $(\mathcal{N}+1)(\mathcal{N}+2)/2$, which is considerably reduced with respect to the first two expansions. This reduction in the size of the matrices for a given $\mathcal{N}$ allows us to increase the value of the upper limit in equation (7), and improve the energy results, widening the r_s-region over which convergence is obtained.

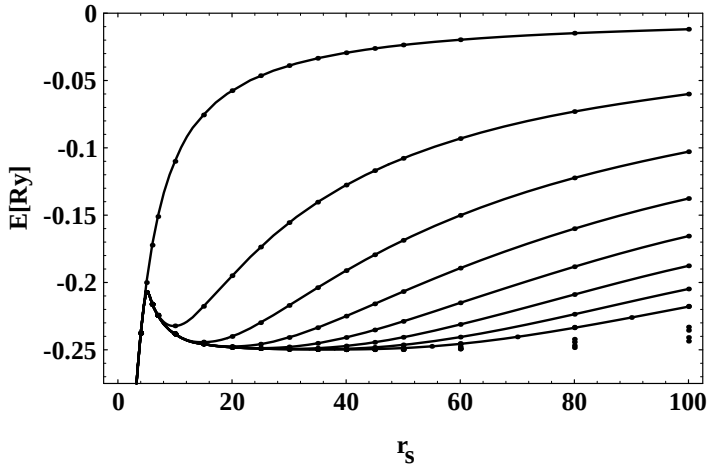

Figure 1. Calculated values of the paramagnetic energy per particle as a function of the Wigner–Seitz parameter, r_s, for the 2D electron gas. The curves correspond to $\mathcal{N} = 0, 4, 8, 12, 16, 20, 24, 28$ from top to bottom. Discrete points correspond to several extrapolations; smaller values come from non-optimized fits.

The energies of the paramagnetic and the ferromagnetic states are evaluated and compared in order to determine the magnetic character of the ground state. The paramagnetic state is a Slater determinant with the functions given by equation (7). In this case each one-electron state with wave vector $\boldsymbol{k}$ within a Fermi *circle* of radius k_F has double occupancy because we have both spin states, so $N = \sum_{k,\lambda} n_{k,\lambda}$ with $n_k = \Theta(k_F - k)$ where Θ is the step function. In the fully polarized ferromagnetic system, each orbital within a circle of radius $\sqrt{2}k_F$ is singly occupied. The ferromagnetic system is an example of anomalous occupancy in spin space characterized by $N = \sum_{k,\lambda} n_{k,\lambda_1}$ with $n_k = \Theta(\sqrt{2}k_F - k)$. Then the Fermi circle radius is k_F in the paramagnetic case and $\sqrt{2}k_F$ in the ferromagnetic one.

Because the DJ depends on a single parameter, a simple rescaling relates the paramagnetic and ferromagnetic states.

In the calculation of the energy, the sums are over occupied states, and we use a Fermi *circle* (disc) occupation approximation. This approximation will induce a fractional occupancy per peak in the corrugated state. A more refined and conceivably better ground state can be obtained if the disc approximation is not used. In the low-density region where the energy is proportional to the Fermi momentum, one expects a correction of the order of 10% or $1 - \sqrt{(}\pi)/2$.

3. Results and discussion

In order to obtain solutions independent of $\mathcal{N}$, calculations were carried out for the electron gas with the expansions for the ground-state function with $\mathcal{N}$ up to 28. The largest matrices that we have to deal with in the basis of equation (7) are of dimension 435. The coefficients C_n were self-consistently determined with an accuracy of 10^{-5} with respect to the last iteration. The paramagnetic results are now discussed. The ferromagnetic energies are obtained with the replacement of r_s by $\sqrt{2}r_s$. The paramagnetic phase energy per particle is displayed in figure 1 in terms of r_s. The curves are for different values of $\mathcal{N}$, from $\mathcal{N} = 0$ for the top curve, in steps of $\Delta\mathcal{N} = 4$, up to $\mathcal{N} = 28$ for the bottom curve. Discrete points correspond to several extrapolations. The curve with $\mathcal{N} = 0$ gives the PW behaviour; in this case the DJ reduces to the UJ. At high densities the paramagnetic HF state of the 2D electron gas is the PW up to $r_{sc} = 4.8$. At this point a symmetry transition from a homogeneous to a localized state occurs. At intermediate and low densities where the transition to the eDW has occurred, the DJ energy of the system with localized solutions is lower than the energy obtained with the UJ and correlated state functions [8].

Table 1. Computed values of the energy per particle for the 2DEG in the paramagnetic phase as a function of the Wigner–Seitz parameter and the number of functions, $\mathcal{N}$, in each physical direction. The last column shows the results of non-linear extrapolations in terms of the parameter $\mathcal{N}$; the numbers in parentheses are estimates of the extrapolation precision in the last significant figure.

	$\mathcal{N}$							
r_s	16	18	20	22	24	26	28	Extrapolation
10	−0.238 21	−0.238 21	−0.238 21	−0.238 21	−0.238 21	−0.238 21	−0.238 21	−0.2382
20	−0.248 09	−0.248 10	−0.248 10	−0.248 10	−0.248 10	−0.248 10	−0.248 10	−0.2481
30	−0.247 88	−0.248 93	−0.249 36	−0.249 52	−0.249 51	−0.249 51	−0.249 51	−0.2495
40	−0.240 85	−0.244 80	−0.247 17	−0.248 52	−0.249 24	−0.249 60	−0.249 75	−0.2498(1)
50	−0.228 90	−0.235 80	−0.240 71	−0.244 10	−0.246 36	−0.247 81	−0.248 71	−0.2494(2)
60	−0.215 10	−0.224 14	−0.231 17	−0.236 54	−0.240 56	−0.243 50	−0.245 61	−0.2484(4)
80	−0.188 30	−0.199 47	−0.208 95	−0.216 94	−0.223 61	−0.229 13	−0.233 66	−0.2439(6)
100	−0.165 56	−0.177 27	−0.187 64	−0.196 79	−0.204 83	−0.211 85	−0.217 96	−0.2359(7)

The value of the parameter r_{sc} at which the solutions transform from eDW to PW will be taken as the melting point. The criterion is similar to that given in reference [10] where the authors consider a charge-density wave instead of close-packed structure. In the present work, the melting point occurs at $r_{sc} = 4.8$ for the paramagnetic gas, while the scaled value $r_{sc} = 6.8$ is obtained for ferromagnetic systems. The transition at this point corresponds to a discontinuity in the density, just as in the 3D case; in this sense a first-order transition is

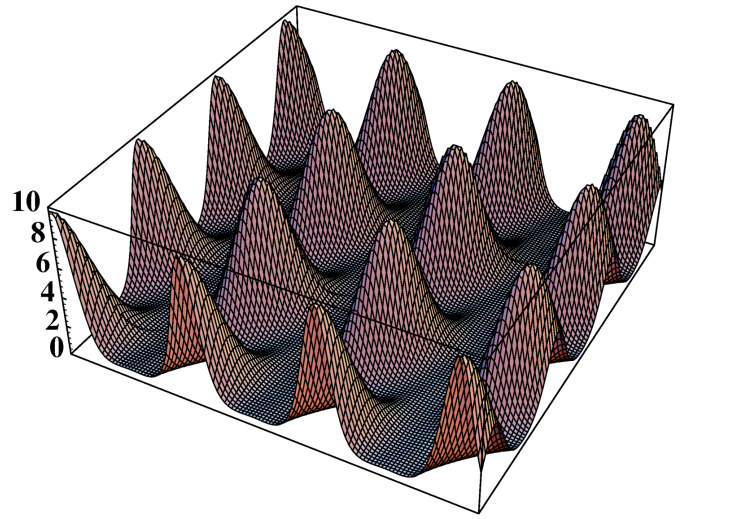

(a)

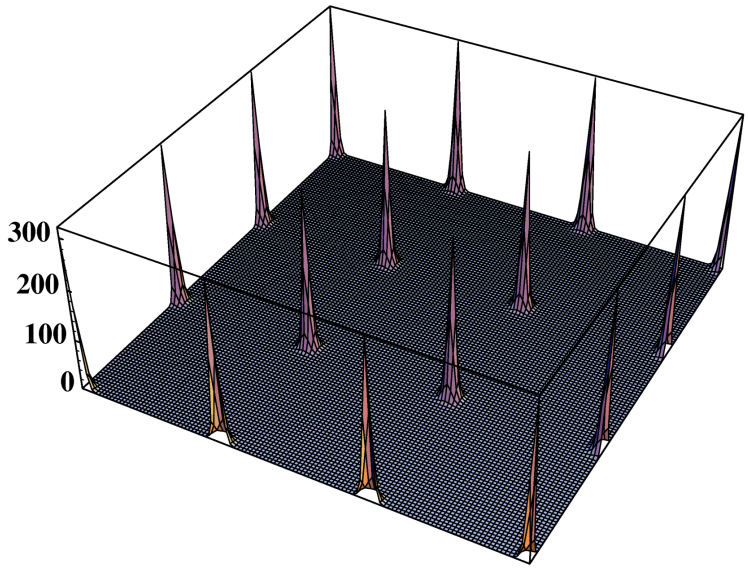

(b)

Figure 2. The electron density normalized to the PW density. (a) For r_s close to the transition; $r_s = 4.8$ for the paramagnetic and $r_s = 6.8$ for the ferromagnetic phase. (b) Far from the transition; at $r_s = 25$ and $r_s = 35.3$ for the paramagnetic and ferromagnetic phases respectively. Notice the change in the vertical scale and the implicit change in the horizontal scale. Horizontal peaks are separated by $2.23r_s$.

(This figure can be viewed in colour in the electronic version of the article; see `http://www.iop.org`)

obtained using the approximations of this work. The electron density normalized to the PW density $\rho(r_s)/\rho_{PW}(r_s)$ in terms of the parameter r_s is shown in figure 2. Two r_s-values are chosen; the first is near the melting points where the electron density is slightly localized,

and the second is at large r_s-values where, according to the Wigner hypothesis [18], the electron density is very pronounced. In figure 2(a), $r_{sc} = 4.8$ for the paramagnetic system and $r_{sc} = 6.8$ for the ferromagnetic one. In figure 2(b), $r_s = 25$ for the paramagnetic and $r_s = 35.3$ for the fully polarized system. The period of the electron density along the axes of corrugation is $L = 2.23r_s$ for the 2D system, as compared with the period for the electron density, obtained in a previous work [19] for the 3D system, of $L_{3D} = 1.63r_s$.

3.1. The stable localized state

For the expansions used in this work with $\mathcal{N} = 28$, good convergence in the paramagnetic state energy is obtained for r_s-values up to 44. An interesting feature of the $\mathcal{N} = 28$ curve is the apparent minimum in the low-densities region, at $r_s \approx 43$. A careful assessment of the existence of this minimum (region of stability) is necessary because of the slow convergence of the series in equation (7). In order to study the behaviour of the energy curve in the region of stability, it is mandatory to achieve convergence in the ground-state energy value over a wider interval of densities. In table 1 the paramagnetic state energy per particle, as a function of r_s and $\mathcal{N}$, is given. As this table shows, the convergence in energy becomes slower when r_s increases, and a greater number of terms are required in the state function. Therefore we have not reached a direct conclusion about the behaviour of the energy curve at low densities ($r_s > 44$). This problem might be solved if we could have a greater number of terms in the state function, or if we could obtain the limit at low densities in an alternative way. Due to the great computational cost of the first alternative, we are forced to adopt the second one.

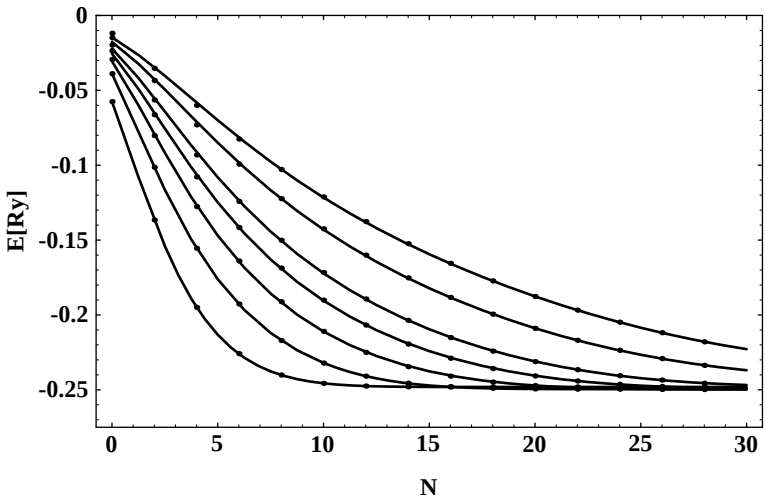

Figure 3. A fit of the calculated data for the electron gas system. The functional form of equation (8) has been used. The curves correspond to $r_s = 20, 30, 40, 50, 60, 80, 100$, the upper curves at low $\mathcal{N}$ corresponding to larger r_s.

We have studied in detail the convergence of the computation. At fixed r_s, we obtain a functional of the form

$$E(\mathcal{N}) = E(\mathcal{N}_0)\exp\left(\int_{\mathcal{N}_0}^{\mathcal{N}} \exp(p_r(x))\ \mathrm{d}x\right) \tag{8}$$

where p_r is a polynomial of degree r with adjustable coefficients. This form gives a very good fit [20] for the range of $\mathcal{N}$-values from 0 to 28 with a polynomial p_r of order $r = 3$. Polynomial forms of smaller degrees tend to give less good fits, and higher-degree polynomials give negligible corrections. Because the fits are used to extrapolate to large $\mathcal{N}$ we have given large weights, of order 300, to the data for $\mathcal{N} \geqslant 20$ as compared to the data for the low values, $\mathcal{N} \leqslant 8$; the size of the weights is comparable to the number of orbitals for a given $\mathcal{N}$. A numerical estimate of the goodness of the fit is obtained from its χ^2-values; typical values of χ^2 vary between 10^{-7} for low r_s and 10^{-5} for $r_s \geqslant 60$. In figure 3 one such fit is shown for the paramagnetic phase; on the basis of the fits an extrapolation to large $\mathcal{N}$ was carried out. The results of the extrapolations are given in figure 1. All of the extrapolations that we have tried indicate the existence of a minimum in the paramagnetic phase in the region $38 < r_s < 48$. The extrapolated energy per particle is very close to -0.25 Ryd at the minimum. For the ferromagnetic phase, equivalent results are obtained in the scaled region $54 < r_s < 68$.

A many-body physical system such as the electron plus the background that we are considering has many modes of oscillation around its ground state. Some of them are density fluctuation modes; one can distinguish two classes of density fluctuation: the first are the charge-density fluctuations, while the second are neutral-density oscillations. Among the charge-density fluctuations we have electron-density fluctuations which go beyond the HF approximation, and, also, background charge fluctuations which correspond to phononic modes in the DJ. The charge-separating modes are expected to have relatively large energies as compared to the neutral-charge oscillations due to the dipole energies that they generate. The size of the neutral modes can be estimated within the DJ from the E/N versus r_s curves, in close analogy with the Born–Oppenheimer procedure for molecular vibrational modes.

The energy per particle depends on a single parameter r_s, which determines the electron *and* background density. A simple harmonic calculation of the energy levels of oscillation around the minimum can be performed. Because the ferromagnetic energy has a lower degree of dependence on r_s than the paramagnetic phase, the elastic energy is smaller for the ferromagnetic than for the paramagnetic case. Let us discuss the paramagnetic case. The energy curve has two minima—one in the high-density region where the well known PW is the HF-DJ solution, and the second in the intermediate-density region, at $r_s \approx 43$, where the DJ has the eDW as the HF state function. We have a harmonic potential, so we ask what object oscillates in it. We assume that it will be a neutral atom. In order to get an upper bound for the correction, we assume the mass of the lightest atom, hydrogen. The vibrational energies of other atoms will scale as $1/\sqrt{A}$, with A the mass number. The excitation energies around the high-density minimum are $\Delta E(r_s \approx 1.66) = 0.9 \times 10^{-2}$ Ryd, and around the low-density minimum $\Delta E(r_s \approx 43) = 0.9 \times 10^{-4}$ Ryd. One notices that ΔE at low densities is much lower than the high-density value; therefore a negligible zero-point energy correction, less than 0.1%, to the low-density curve is expected from this effect. Therefore the 2D metastable localized state is stable against these deformations.

There are other criteria for stability, which are related to the behaviour of the pressure and bulk modulus [22]. The pressure depends on the negative of the first derivative of the energy:

$$p = -\frac{1}{8\pi}\frac{\mathrm{d}\epsilon}{\mathrm{d}r_s}$$

where ϵ is E/N. Beginning at the melting point and extending up to $r_s \approx 43$ in the paramagnetic phase and up to $r_s \approx 61$ in the ferromagnetic phase, we have a region of

positive pressure. The bulk modulus or inverse compressibility is given by

$$B = 1/\kappa = \frac{1}{16\pi}\left[\frac{\mathrm{d}^2\epsilon}{\mathrm{d}r_s^2} - \frac{1}{r_s}\frac{\mathrm{d}\epsilon}{\mathrm{d}r_s}\right]$$

in the 2D case. At intermediate and low densities, the bulk modulus in our model is positive from the melting point up to densities of $r_s \approx 80$ and $r_s \approx 115$ for the paramagnetic and ferromagnetic phases respectively. The high-density region where the PW is the HF-DJ ground state is well known. Notice that these properties depend only on the parameter r_s, retaining the simplicity of the jellium model.

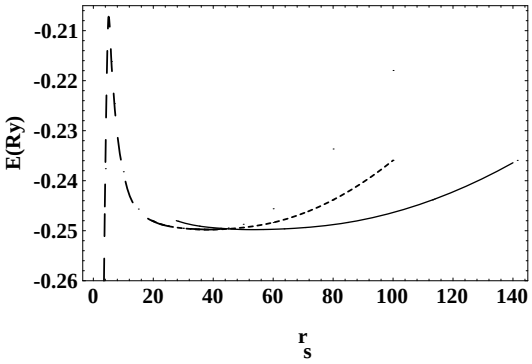

Figure 4. The ground-state energy per particle for the 2DEG in terms of r_s. The results with $\mathcal{N} = 28$ were obtained at intermediate densities, and the extrapolated ones were obtained at low densities. The dashed curves are the paramagnetic phase energies and the continuous curves correspond to the ferromagnetic ones. From $r_s \approx 2$ up to $r_{st1} \approx 6.6$ the FPW solutions are the DJ ground state. From $r_s \approx 6.6$ up to $r_{st1} \approx 42$ a paramagnetic localized state is predicted. At $r_{st2} = 42$ the electron gas exhibits a transition to a ferromagnetic localized configuration.

3.2. The ground state of the 2DEG

In figure 4 the $\mathcal{N} = 28$ paramagnetic and ferromagnetic energies as functions of r_s are shown in order to display the magnetic character of the ground state for the 2D electron gas system. The dashed curves are for the paramagnetic phase energy, and the continuous curves are for the ferromagnetic one. The small-dashed curve represents the extrapolated paramagnetic energy, and the large-dashed curve represents the non-magnetic energy evaluated with the state function with $\mathcal{N} = 28$. These two curves separate at $r_s \geqslant 44$. The thick continuous curve gives the HF ferromagnetic energies, and at $r_s \geqslant 65$ it separates from the thin continuous curve which represents the extrapolated ferromagnetic energy. As the transition from the paramagnetic PW (PPW) to the ferromagnetic PW (FPW) is well known, we will not discuss it. From $r_s \approx 2$ up to $r_{st1} \approx 6.6$ the FPW solution is the HF ground state of the 2D electron gas in the DJ. At this point a magnetic and symmetry transition to a paramagnetic localized state is predicted. In this phase a positive-pressure region is obtained up to $r_s \approx 43$. Then at $r_{st2} = 42$ the electron gas undergoes a magnetic transition to a ferromagnetic localized configuration, and a new positive-pressure region is observed in this phase up to $r_s \approx 61$. Thanks to the improved basis and the extrapolated results, the value for the latter transition point is better determined than in previous work [15]. As the extrapolation shows, at very low densities the ground state is a Wigner crystal in the ferromagnetic phase; a similar result was obtained for the 3D electron gas in the DJ

model [14]. While in reference [9] the paramagnetic state has the lowest energy at all densities, in reference [8] the ferromagnetic state has lower energy than the paramagnetic state at low densities ($r_{st} \geqslant 40$), as in the present work ($r_{st} \geqslant 42$). Once the transition to the eDW has happened (at r_{st1}), the pressure is positive from $r_s \approx 6.6$ up to $r_s \approx 61$. The bulk modulus remains positive from $r_s \approx 6.6$ up to larger values, $r_s \approx 115$.

The ground state's melting point in this work is $r_{st1} \approx 6.6$. In reference [21] the authors find that the Wigner lattice becomes unstable due to quantum fluctuations at $r_{sc} < 5.57$, whereupon the instability is triggered by dislocations; this result is very close to ours. Also interesting is the result in reference [17] where the authors get $r_{sc} \approx 8$ as the transition point at which the crystalline-state energies are lower than the gaseous-state energies. Notice that the energy per particle in the corrugated region, obtained with variational Wannier functions in terms of Gaussian orbitals, is a constant for this calculation [17], and is higher than our calculated result. The latter transition values are significantly smaller than the results for the 2D electron gas obtained using the density functional method, where $r_{sc} \approx 18$, as reported in reference [10], and using the GFMC method, in the UJ [8], where $r_{sc} \approx 37$.

One must be cautious in comparing the UJ or the DJ with experiments. The reason for this is that in the experimental set-up the background is spatially separated from the electronic charges. However, the substrate into which the electronic charge is deposited is expected to react. In the case of a 'metallic' substrate, one expects image charges to develop, simulating the DJ model background deformation; in the case of a dielectric substrate, at least some polarization must occur, and one would expect a situation intermediate between the UJ and the DJ to be physically adequate.

In order to make a comparison with available experimental data, one must take into account effects beyond the HF approximation. A minimal correction that fits naturally in the jellium models is that of modifying the mass into an effective-mass term, m^*, and taking into account electron-charge-screening effects via a dielectric constant, ϵ. Notice that the effective mass and the dielectric constant introduced constitute the static approximation to many-body effects that are independent of the DJ model. In terms of diagrams, m^* and ϵ come from the self-electron-mass and *photon*-mass corrections, respectively. The UJ and DJ depend on a single dimensionless parameter, r_s. Thus physical measures like the energy and the Bohr radius are simply rescaled in terms of the effective electron mass and the dielectric constant. These particular rescalings are $E_B^* = (m^*/\epsilon m)E_B$ with $E_B = e^2/2a_0$ and $a_0^* = (\epsilon m/m^*)a_0$ where $a_0 = \hbar^2/me^2$. Using these equations we can immediately relate the present work to experimental data, and compare its predictions with other theoretical models on the Wigner crystallization. In the case of the Si MOSFET, an electron crystal can be formed under quantum-mechanical conditions even at *zero magnetic field* (magnetic fields so weak that the Landau levels are not resolved). Taking the values $m^* = 0.2$ and $\epsilon = 7.8$, one gets a density for the transition to the localized phase of the ground state of $n_{DJ} = 1.92 \times 10^{11}$ cm^{-2}. Then the DJ melting density for Si inversion layers is of the same order of magnitude as the observed experimental transitions $n_{\mathrm{Si}} \approx 10^{11}$ cm^{-2} [4], which is a remarkable result for a DJ approach. Additional correlation effects beyond the static approximation could possibly improve the agreement with experiment, because the phase transition points are expected to change.

4. Conclusions

Ground-state properties of the 2DEG at zero magnetic field have been obtained by means of HF-DJ self-consistent calculations. This method describes the high-, intermediate-, and low-density regions in a unified fashion. A technique that exploits the symmetries of the

ground-state wave function was applied. This technique allows a considerable size reduction of the Hamiltonian matrix to be achieved, and dramatically improves the reliability, the convergence, and the computational time required for the calculation. Despite all this, in the low-density region above $r_s = 62$, convergence could not be obtained, and an extrapolation of the energy results has been carried out. This extrapolation gives reasonable control of the low-density results. The functional form in equation (8) of the extrapolation gives an extremely good fit to the data once a non-linear functional is selected. This functional form itself recalls those obtained using the renormalization group in many-body theory. The most interesting result is the existence of the stability regions obtained for the energy curve for the 2D electron gas. On the basis of the extrapolation method, two minima are expected in the energy curve at low densities: at $r_s \approx 43$ in the localized paramagnetic phase, and at $r_s \approx 61$ in the localized ferromagnetic one. Thus two metastable states have been found. In principle, they provide a starting point for more sophisticated calculations.

The theoretical value of the ground state's melting point for the Wigner crystal in this work, $r_s = 6.6$, is of the same order of magnitude as the transition values obtained using other models. With the appropriate dielectric constant and effective mass, the melting transition of Si inversion layers is obtained in the order of magnitude of the experimental results. We think that taking into account correlation effects beyond the static approximation will move the melting point to larger r_s-values, or equivalently to smaller density values, which will give better agreement with experiment.

The expansion for the state function proposed in this work is such that the system can present an electron density centred around a square lattice. Once the symmetry of the basis is chosen, the $N \to \infty$ basis is complete for the ground state. That the odd (sine) part of the Fourier series does not contribute has been checked up to $N \approx 10$. Other lattices can be obtained by the usual modification of the Brillouin-zone geometry. Although in the 2D system one expects that the hexagonal lattice will be the most favourable energetically, we obtain that, even for the square lattice, the DJ gives a lower energy (a more stable system) than the corresponding UJ calculations which include correlations. This fact suggests that important background effects might have been underestimated in the UJ. The DJ calculations suggest that a large deviation of the UJ might be favoured at intermediate and low densities.

Acknowledgment

This work was partially supported by the Consejo Nacional de Ciencia y Tecnología, México, Project Numbers 5-4330 PE and 3097 P-E.

References

[1] Bauer G, Kuchar F and Heinreich H (ed) 1984 *Two-dimensional Systems, Heterostructures and Superlattices* (Berlin: Springer)
Sivan J U, Solomon P M and Shtrikman H 1992 *Phys. Rev. Lett.* **66** 674
Einspruch N G and Fresley W R (ed) 1994 *Heterostructures and Quantum Devices* (London: Academic)
[2] Micnas R, Ranninger J and Robaszkiewics S 1990 *Rev. Mod. Phys.* **62** 113
Méndez-Moreno R M, Moreno M, Orozco S and Ortíz M A 1993 *Mod. Phys. Lett.* B **7** 1601
[3] Abstreiter G, Brugger H, Wolf T, Zachai R and Zeller Ch 1986 *Physics and New Devices* ed G Bauer, F Kuchar and H Heinreich (Berlin: Springer)
[4] Pudalov V M, D'Iorio M and Campbell J W 1994 *Physica* B **194–196** 1289
D'Iorio M, Pudalov V M, Kravchenko S V and Campbell J W 1994 *Surf. Sci.* **305** 115
D'Iorio M, Pudalov V M and Semenchinsky S G 1990 *Phys. Lett.* **150A** 422
[5] Glattli D C, Deville G, Duburcq V, Williams F I B, Paris E, Etienne B and Andrei E Y 1990 *Surf. Sci.* **229** 344

[6] Furneaux J E, Kravchenko S V, Mason W, Pudalov V M and D'Iorio M 1996 *Surf. Sci.* **361+362** 949
[7] Senatore G and March N H 1994 *Rev. Mod. Phys.* **66** 445
[8] Tanatar B and Ceperley D M 1989 *Phys. Rev.* B **39** 5005
[9] Sim Hock-Kee, Tao R and Wu F Y 1986 *Phys. Rev.* B **34** 7123
[10] Sander L M, Rose J H and Shore H B 1980 *Phys. Rev.* B **21** 2739
[11] Overhauser A W 1968 *Phys. Rev.* **167** 691
[12] Barrera R, Grether M, de Llano M, Peltier S and Plastino A 1979 *J. Phys. C: Solid State Phys.* **12** L715
[13] Oh In-Keun, Mahanty J and Das M P 1994 *J. Phys.: Condens. Matter* **6** 4897
[14] Méndez-Moreno R M, Ortíz M A and Moreno M 1989 *Phys. Rev.* A **40** 2211
[15] Méndez-Moreno R M, Moreno M and Ortíz M A 1991 *Phys. Rev.* A **44** 2370
[16] Méndez-Moreno R M and Ortíz M A 1986 *Rev. Mex. Fis.* **32** 413
[17] Iyakutti K and Rajeswara Palanichamy R 1994 *Int. J. Quantum Chem.* **51** 329
[18] Wigner E P 1938 *Trans. Faraday Soc.* **34** 678
[19] Orozco S, Ortíz M A and Méndez-Moreno R M 1992 *Phys. Rev.* B **46** 13 073
[20] Wolfram S 1991 *Mathematica* 2nd edn (Redwood City, CA: Addison-Wesley)
[21] Chang Mau-Chung and Maki K 1983 *Phys. Rev.* B **27** 1646
[22] Ichimaru S 1982 *Rev. Mod. Phys.* **54** 10 171
Iwamoto N 1982 *Phys. Rev.* A **30** 3289
Rose J H and Shore H B 1994 *Phys. Rev.* B **49** 11 588
Perdew J P, Tran H Q and Smith E D 1990 *Phys. Rev.* B **42** 11 627